Control of Periodic Nanostructure Embedded in SiO_2 Glass under Femtosecond Double-Pulse Irradiation

Atsushi Murata[1], Yasuhiko Shimotsuma[*1], Masaaki Sakakura[2], Kiyotaka Miura[1]

[1]*Department of Material Chemistry, Graduate School of Engineering, Kyoto University, Kyoto 615-8510, Japan*
**yshimo@func.mc.kyoto-u.ac.jp*
[2]*Society-Academia Collaboration for Innovation, Kyoto University, Kyoto 606-8501, Japan*

The polarization-dependent periodic nanostructure are successfully induced by the femtosecond double-pulse train. Such nanograting structures consist of periodic modulation of oxygen deficiency with nanoscale. Furthermore, we have also observed that this stripe-like oxygen defect regions include nanopores. Additionally, the average size of the induced nanopores by the double-pulse train was twice as large as that of the single-pulse train, despite of the same total energy. As the results, twice higher birefringence can be obtained by the double-pulse train irradiation.

DOI: 10.2961/jlmn.2016.01.0018
Keywords: SiO_2 glass, femtosecond laser, double-pulse train, nanostructure, anisotropy

1. Introduction

The interaction between femtosecond laser pulses and transparent materials has been investigated by many researchers in recent years [1-12]. As one of the intriguing phenomenon for SiO_2 glass, the formation of nanogratings (NGs) in the focal volume is known [8-11]. Nanogratings consist of the periodic modulation of oxygen deficiencies with nanoscale in glass, which are self-assembled in the direction perpendicular to the laser polarization. As the results, the form birefringence can be observed by the formation of nanogratings in an isotropic material, namely glass. The origin of the birefringence is interpreted by the creation of oxygen deficiencies and the nanopores, leading to the periodic modulation of low density material with a scale of subwavelength [13]. Such nanograting structures are useful for the applications to a five-dimensional optical storage [10] and a polarization imaging in real-time [11]. In order to realize such innovative application, higher birefringence is expected for the low threshold and the energy efficiency. Until now, we have proposed the mechanisms of the self-organization based on the interference between the electric field of the incident light and the generated electron plasma wave [8]. Whereas, another group has also proposed the formation mechanism of nanoplanes due to nanoplasmonic effects [14]. More recently, Canning et al. reported that the NGs consist of oxygen defects are formed via self-trapped excitons (STEs) [15]. However, the detail of the oxygen defects dynamics is not fully understood. In this work, we focused on the formation dynamics of NGs under the irradiation of the femtosecond double-pulse train. We have evaluated the localized form-birefringence in SiO_2 glass induced by the femtosecond double-pulse train with various delay times. From the results of double-pulse train experiments modulated by the acoustic optic phase dispersion filter (AOPDF), the phase retardation induced by the double-pulse train with up to 5 ps delay was larger than that of the conventional single pulse train [16]. We have also measured the phase retardation induced by the double-pulse train with longer delay time (up to 1700 ps) compared to the lifetime of STEs.

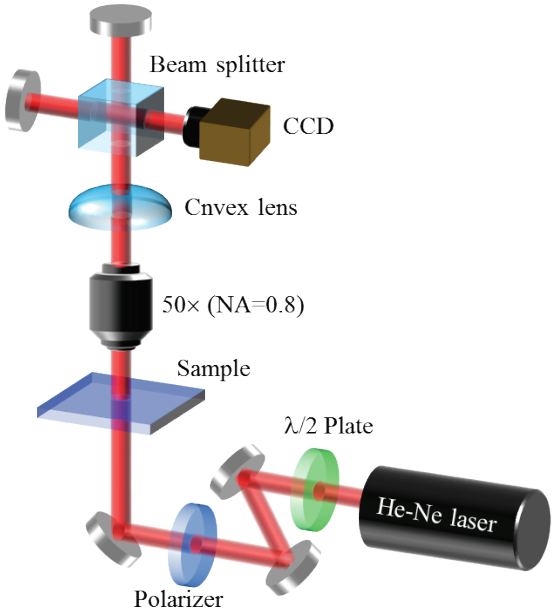

Fig. 1 Schematic of the interferometer for measurement of the phase shift in the modified regions.

2. Experimental

The experiments were performed using a mode-locked, regeneratively amplified Ti: Sapphire laser system (Coherent; RegA 9000), operating at 800 nm with 50 fs pulse duration, and a laser beam was equally split by a polarizing beam splitter. The polarization of the beams was the same polarization (E = 90°). The delay time, τ_{delay}, between parallelly polarized double-pulses, ranging from 1 ps to 1700 ps, was varied using an optical delay line. Finally both beams were recombined on the second polarizing beam splitter. The laser beam was focused via a microscope objective (Nikon; LU Plan Fluor, 50× 0.80 N.A.) at a depth of about 100 μm below the surface of SiO_2 glass sample (Shinetsu Chemical Corp.; VIOSIL-SQ). The

pulse energy (E_{pulse}) was 0.5 μJ and the beam power measured after microscope objective was independent on the orientation of light polarization. The repetition rate (R) of the laser was set to 10 ~ 250 kHz corresponding to an interpulse time of τ_{int} = 4 ~ 100 μs. The total number of pulses was adjusted through the translation velocity of 10 ~ 250 μm/s (corresponding to 1000 pulses within focal diameter).

The modified regions was inspected by a polarization microscope (CRi Inc.; LC-Polscope) and for evaluation of the induced phase retardation. To reveal structural changes, the modified regions also observed by scanning electron microscopy (JEOL; JSM-6705F). Using a scanning electron microscope (HITACHI, SU8000) without deposition of the conductive coating, we analyzed the cleaved surfaces including laser writing regions by the femtosecond pulses with a polarization direction parallel to the scanning direction. To evaluate the refractive index change and the form-birefringence in the modified regions, we constructed a Michelson interferometer (Fig. 1). We measured the index change based on the phase shift of the transmitted light [17].

3. Results and discussion

Fig. 2 shows the variation of the phase retardation depending on the τ_{delay} for each repetition rate. According to longer τ_{delay}, the phase retardation starts to decrease at 10 ps and then, after 600 ps, asymptotically reaches the retardation value for the half laser energy (E_{pulse} = 0.25 μJ). Interestingly, the phase retardation for double-pulse train was twice as large as that for single-pulse train, despite of the same total energy. The optimal interpulse time of τ_{int} to achieve maximum phase retardation was 20 μs corresponding to R = 50 kHz. Assuming the excessive thermal accumulation in the case of τ_{int} < 20 μs, smaller phase retardation value could be interpreted in terms of the annihilation of oxygen deficiencies and/or nanopores, leading to the quality deterioration of the NGs [10]. On the other hand, a reason of the smaller phase retardation for τ_{int} > 20 μs is not clear. We have speculated that the oxygen deficiencies and nanopores were also induced by the thermal effect during laser irradiation.

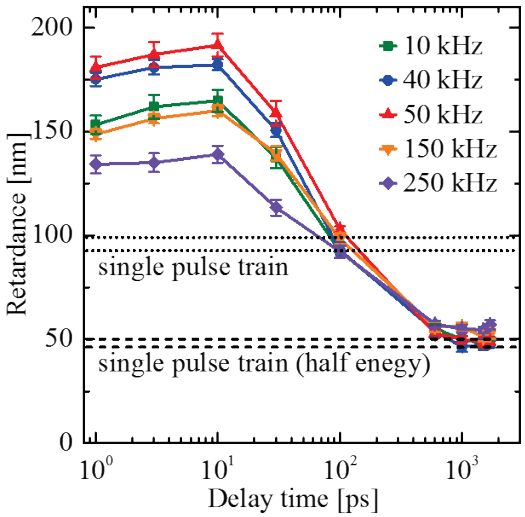

Fig. 2 Variation of the phase retardation as a function of the τ_{delay} for each repetition rate.

Considering the energy diagram of glass after the femtosecond double-pulse train irradiation (Fig. 3), these results suggest that a free electron produced by the first arriving pulse has been relaxed within 10 ps and trapped at STEs [18]. The trapped electrons at STEs can interact with the second arriving pulse when a τ_{delay} is appropriate, owing to the slow STEs decay (several hundred picoseconds).We considered that the re-ionized process became easy to be caused and thereby the total oxygen defects increased in this time scale. Finally, after 600 ps, the number of electrons in the STEs level, which can interact with the second arriving pulse, decreases with increasing τ_{delay}, and asymptotically reaches the value in the case of the single-pulse train.

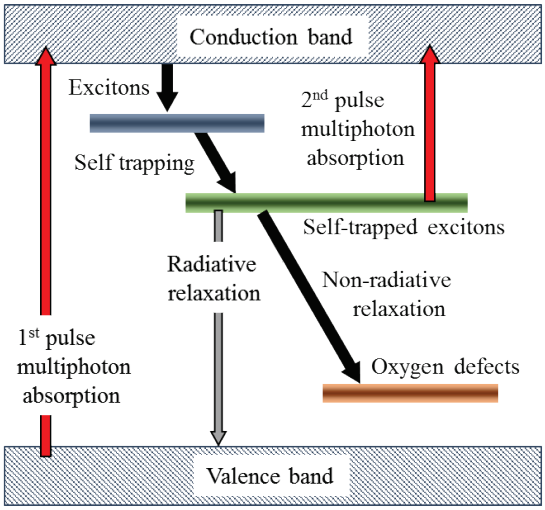

Fig. 3 Schematic of the dynamics model of oxygen defects generation in SiO_2 glass.

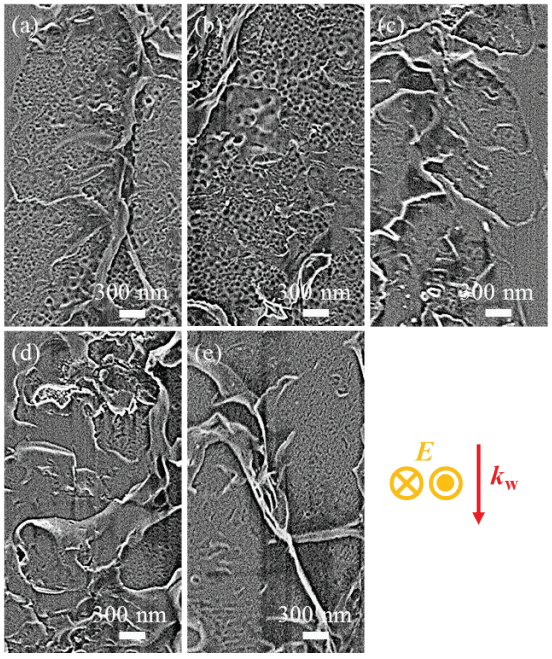

Fig. 4 SEIs on the cleaved surface of laser traces written by femtosecond double-pulse train with τ_{delay} = (a) 1 ps, (b) 10 ps, (c) 100 ps and (d) 1000 ps. The result on the single pulse train is also shown in (e). E and k_w show the polarization direction and the laser propagation direction. The laser parameters were as follows: 800 nm, 50 fs, 0.5 μJ, 50 kHz, 1000 pulses/μm, 0.80NA.

In order to reveal the interaction between the electrons, which are excited by the first arriving pulse, and the second arriving pulse, we observed the cleaved surface of the modified regions. Fig. 4 shows secondary electron images (SEIs) on the cleaved surface of the laser races written by double-pulse train (τ_{delay} = 1, 10, 100, 1000 ps) or single-pulse train with total pulse energy (E_{total}) of 0.5 μJ at R = 50 kHz. We observed nanopores in each cleaved surface of the laser traces, and then estimated their diameter (d) and occupation area ratio (ψ) by the image processing (Fig. 5).

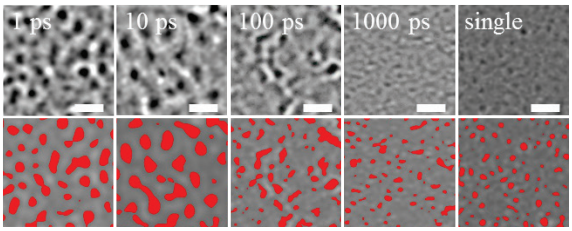

Fig. 5 (Upper row) High magnification SEIs for each photos in Fig. 4. (Bottom row) Images processed by the image processing algorithm in order to recognize nanopores for each photos in upper row. Scale bars are 100 nm.

The evaluated results were listed in Table 1. Compared between the fluctuation of the phase retardation (Fig. 2) and the changes in parameters of nanopores (Table 1) according to the τ_{delay} of double-pulses, we found that these are correlated. These results indicate that, depending on the interpulse time, the quantity of the induced oxygen deficiencies and nanopores are controllable. In particular, we considered that the size of a nanopore and its vacancy existence ratio are dominant factors in the photoinduced birefringence.

Table 1 The diameter of nanopores (d) and the occupation-area-ratio (ψ) obtained by the image processing of SEIs.

	Double-pulse train				Single-pulse train
τ_{delay} [ps]	1	10	100	1000	-
d [nm]	31	46	22	12	19
ψ [%]	30	38	18	10	16

Using the home-made interferometer system, we have also measured the refractive index changes induced by double-pulse train (E_{pulse} = 0.5 μJ, τ_{delay} = 10 ps, τ_{int} = 20 μs) and single-pulse train (E_{pulse} = 0.5 μJ, τ_{int} = 20 μs). The measurements were summarized in Table 2.

Table 2 Results of the interferometer measurement for the local refractive index changes induced by the femtosecond double-pulse train or single-pulse train.

Parameter	Double-pulse train	Single-pulse train
L [μm]	15	15
δ_x	-3.11	-1.625
δ_y	-0.915	-0.589
n_x	1.439	1.448
n_y	1.454	1.455
Δn	0.015	0.007

Moreover, we have also calculated the birefringence based on these measurements. The birefringence for ordinary (n_x) and extraordinary (n_y) wave is as follows [19]:

$$\Delta n = \left(n_y - n_x\right) = \left[f n_1^2 + (1-f) n_2^2\right]^{0.5} - \left[\frac{n_1^2 n_2^2}{f n_2^2 + (1-f) n_1^2}\right]^{0.5} \quad (1)$$

where f is the filling factor, n_1 and n_2 are the unknown refractive index for the plates constituting the NGs (Fig. 6).

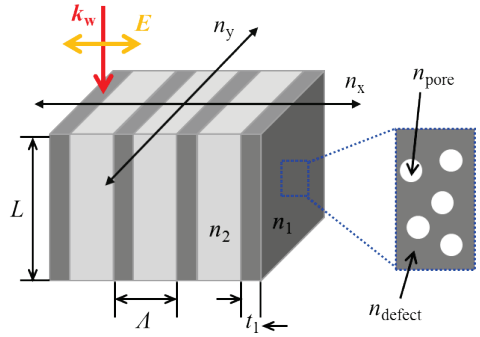

Fig. 6 Schematic of the nanogratings structure for the estimation of the photoinduced birefringence.

The NGs are ruled in the direction parallel to the polarization of the writing laser, and consist of thin regions of refractive index n_1, characterized by a strong oxygen deficiencies surrounded by larger regions of index n_2 [8]. In addition, based on the Maxwell-Garnett theory, the effective refractive index (n_1) of the mesoporous planes with the thickness of 50 nm for SiO_2 glass is given as:

$$n_1^2 = n_{defect}^2 \left[1 - \frac{3\phi\left(n_{defect}^2 - n_{pore}^2\right)}{2n_{defect}^2 + n_{pore}^2 + \phi\left(n_{defect}^2 - n_{pore}^2\right)}\right] \quad (2)$$

where ϕ is the porosity, n_{pore} (= 1) and n_{defect} are the local refractive indices for the nanopores and for the surrounding oxygen defect regions, respectively. The thickness (t_1) of the regions with refractive index of n_1 was estimated to be 50 nm or 20 nm for double-pulse train or single-pulse train, respectively (Fig. 7).

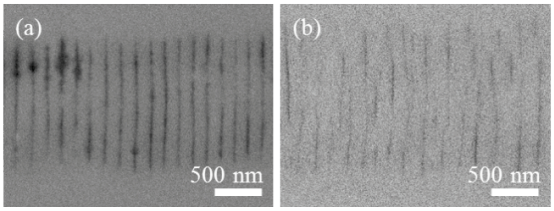

Fig. 7 The BEIs on the polished sample surfaces to the depth of the nanogratings induced by the femtosecond direct writing (a) with the double-pulse train (E_{total} = 0.5 μJ, τ_{delay} = 10 ps, τ_{int} = 20 μs) or with the single-pulse train (E_{pulse} = 0.5 μJ, τ_{int} = 20 μs).

Table 3 Parameters for calculation of local refractive index changes induced by the double-pulse train or single-pulse train.

Parameter	Double-pulse train	Single-pulse train
t_1 [nm]	50	20
Λ [nm]	200	200
$f = t_1/\Lambda$	0.25	0.10
ϕ	0.35	0.20
Δn	0.011	0.004

We assumed that these thicknesses correspond to the diameter of nanopores. Assuming that the porosity, ϕ in the

regions with refractive index n_1 is 0.35 or 0.20 for double-pulse train or single-pulse train (Fig. 5), the birefringence could be obtained (Table 3). Comparison between Table 2 and Table 3 indicates that the birefringence value obtained from the two different methods is in good agreement.

Meanwhile, the generation of molecular oxygen confined in a nanovoids inside glass was observed inside bulk glass of SiO_2 [13] and GeO_2 [20]. It should be considered that the molecular oxygen was produced by the recombination of oxygen atom dissociated from the glass network structure before the structure freezing. Based on the fact that the nanopores of the mesoporous planes in which oxygen defects exist were disappeared after the annealing at 1200 °C for 1h, the pressure inside nanopores was assumed to be negative. While, Bressel et al. suggested that molecular oxygen might be formed in the void long after the pulse end in a relatively cool state [20]. Their conjecture is qualitatively in agreement with the experimental results at higher laser fluence. Higher fluence means higher temperature, higher gradient of oxygen concentration, thus more oxygen diffused into the void. We have observed FT-IR spectra before and after the irradiation of femtosecond single-pulse train or double-pulse train (Fig. 8). There are two typical peaks at 3600 cm^{-1} and 2260 cm^{-1} attributed to the Si-O-H stretching vibration (ν_1) and the overtone mode of the Si-O-Si bond-stretching vibration (ν_2), respectively. In order to discuss the peak intensity qualitatively, we measured IR spectra of the same glass sample passed through the iris of 1 mm. The laser tracks with a size of 2 × 2 mm written by both of single- and double-pulse trains consists of a line and space pattern (~ 1.5 μm / 2 μm). It is known that the fictive temperature of glass was empirically obtained by the following equation [21]:

$$T_f = \frac{43809.21}{\nu_2 - 2228.64} \tag{3}$$

where ν_2 [cm^{-1}] is the peak position at about 2260 cm^{-1} and T_f is the fictive temperature. In our case, no apparent peak shift at 2260 cm^{-1} was observed. On the other hand, the peak intensity of ν_1 at about 3600 cm^{-1} slightly increased by the laser irradiation. Furthermore, larger peak intensity of ν_1 corresponding to higher oxygen concentration was observed in the case of the double-pulse train, compared to the single-pulse train.

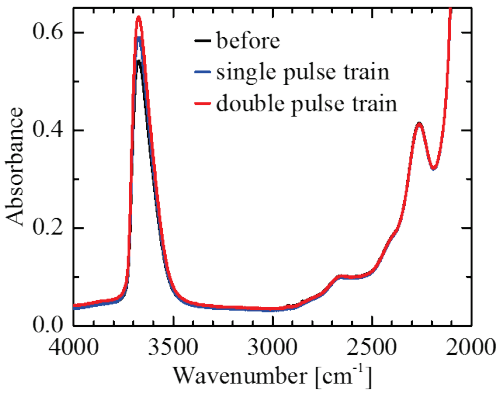

Fig. 8 FT-IR spectra before and after the irradiation of femtosecond single-pulse train (E_{pulse} = 0.5 mJ, τ_{int} = 20 μs) or double-pulse train (E_{total} = 0.5 mJ, τ_{delay} = 10 ps, τ_{int} = 20 μs).

While, Bressel et al. have also observed the thermal quenching effect by the femtosecond laser irradiation [23]. They calculated the fictive temperature from the Raman peak shift of the main band at about 450 cm^{-1} resulting from the symmetric stretching mode of bridging oxygen [24]. Furthermore, assuming that larger pores induced by the double-pulse train simply mean that higher temperatures were reached and faster quenched, it is possible to estimate the formation of the denser phase in the laser writing region. To reveal this assumption, we have also observed the Raman spectra of the glass sample embedded the nanograting structure induced by the femtosecond laser writing with the single-pulse train (E_{pulse} = 0.5 μJ, τ_{int} = 20 μs) or with the double-pulse train (E_{total} = 0.5 μJ, τ_{delay} = 10 ps, τ_{int} = 20 μs). Typical Raman peaks at about 450 cm^{-1}, 490 cm^{-1}, 605 cm^{-1} and 800 cm^{-1} were detected. Defect lines D1 at 490 cm^{-1} and D2 at 605 cm^{-1} are attributed to four- and three-membered rings, respectively [25]. In addition, the 800 cm^{-1} band is attributed to the bending vibration of the Si-O bonds [26]. Since the Raman peak ratio of A_{D2}/A_{tot} is proportional to the fictive temperature [24], we have also calculated the A_{D2}/A_{tot} after the normalization by the 800 cm^{-1} peak area. Where, A_{D2} and A_{tot} are the D2 peak area and the whole Raman peak area, respectively. Although no apparent peak shift at about 450 cm^{-1} was observed in our case, the A_{D2}/A_{tot} is larger for the laser writing with the double-pulse train than with the single-pulse train, corresponding to a higher fictive temperature for the initial glass. To sum-up, the results of FT-IR and Raman spectra indicate that the generation of the more oxygen molecules and the denser phase was induced by the femtosecond double-pulse train. This is qualitatively in agreement with the measurement results of the form birefringence. Further studies including the measurement of the pressure in nanopores are required to understand this phenomenon.

4. Conclusion

In summary, we have observed that the stripe-like regions, which are low density compared to surrounding regions due to the existence of large amount of nanopores, induced by femtosecond double-pulse or single-pulse. Despite of the same total pulse energy, the average sizes of nanopores created by the single-pulse and the double-pulse trains were about 19 nm and 46 nm, respectively. This result indicates that the twice as high phase retardation can be induced by the double-pulse train compared to the single-pulse train. Moreover, we found that the change of induced nanopores by double pulse train of changing τ_{delay} is similar to the tendency to increase and decrease of retardance (Fig. 2 and Fig. 4). Taking account of the relatively longer relaxation time of STE and the results of our double-pulse experiments, we speculate that the re-ionization process probably contributes to the increase of the oxygen defects.

Acknowledgements

This work was partially supported by JSPS KAKENHI Grant Number 26630129, The Thermal & Electric Energy Technology Foundation, Tokuyama Science Foundation, Cross-Ministerial Strategic Innovation Promotion (SIP) Program and Industry-Academia Collaborative R&D Programs (Super Cluster Program).

References

[1] K. M. Davis, K. Miura, N. Sugimotzo, and K. Hirao: Opt. Lett., 21, (1996) 1729.
[2] K. Miura., J. R. Qiu, H. Inouye, T. Mitsuyu, and K. Hirao: Appl. Phys. Lett., 71, (1997) 3329.
[3] C. B.Schaffer, N. Nishimura, E. N. Glezer, A. M. T. Kim, and E. Mazur: Opt. Express, 10, (2002) 196.
[4] A. M. Streltsov and N. F. Borrelli: J. Opt. Soc. Am. B., 19, (2002) 2496.
[5] C. B. Schaffer, A. Brodeur, and E. Mazur: Meas. Sci. Technol., 12, (2001) 1784.
[6] J. W. Chan, T. R. Huser, S. H. Risbud, and D. M Krol: Appl. Phys. A., 76, (2003) 367.
[7] H. Zhang, S. M. Eaton, and P. R. Herman: Opt. Express, 14, (2006) 4826.
[8] Y. Shimotsuma, P. G. Kazansky, J. Qiu, and K. Hirao: Phys. Rev. Lett., 91, (2003) 247405.
[9] Y. Shimotsuma, K. Hirao, J. Qiu, and P. G. Kazansky: Mod. Phys. Lett. B., 19, (2005) 225.
[10] Y. Shimotsuma, M. Sakakura, P. G. Kazansky, M. Beresna, J. Qiu, K. Miura, and K. Hirao: Adv. Mater., 22, (2010) 4039.
[11] Y. Shimotsuma, K. Miura, and K. Hirao: Int. J. Appl. Glass Sci., 4, (2013) 182.
[12] E. N. Glezer, M. Milosavljevic, L. Huang, R. J. Finlay, T. H. Her, J. P. Callan, and E. Mazur: Opt. Lett., 21, (1996) 2023.
[13] M. Lancry, B. Poumellec, J. Canning, K. Cook, J.-C. Poulin, and F. Brisset: Laser Photonics Rev., 6, (2013) 953.
[14] V. R. Bhardwaj, E. Simova, P. P. Rajeev, C. Hnatovsky, R. S. Taylor, D. M. Rayner, and P. B. Corkum: Phys. Rev. Lett., 96, (2006) 057404.
[15] J. Canning, M. Lancry, K. Cook, A. Weickman, F. Brisset, and B. Poumellec: Opt. Mater. Express, 1, (2011) 998.
[16] Y. Shimotsuma, T. Asai, M. Sakakura, and K. Miura: J. Laser Micro/Nanoeng., 1, (2014) 31.
[17] M.Takeda, H. Ina, and S. Kobayashi: J. Opt. Soc. Am.,72, (1982) 156.
[18] S. Richter, F. Jia, M. Heinrich, S. Döring, U. Peschel, A. Tünnermann, and S. Nolte: Opt. Lett., 37, (2012) 482.
[19] T. Asai, Y. Shimotsuma, T. Kurita, A. Murata, S. Kubota, M. Sakakura, K. Miura, F. Brisset, B. Poumellec, and M. Lancry: J. Am. Ceram. Soc., 5, (2015) 1471.
[20] L. Bressel, D. de Ligny, E. G. Gamaly, A. V. Rode and S. Juodkazis: Opt. Mater. Express 1, (2011) 1150.
[21] A. Agarwal, K. M. Davis and M. Tomozawa: J. Non-Cryst. Solids 185, (1995) 191.
[22] L. Bressel, D. de Ligny, C. Sonneville, V. Martinez, V. Mizeikis, R. Buividas and S. Juodkazis: Opt. Mater. Express 1, (2011) 605.
[23] C. Martinet, V. Martinez, C. Coussa, B. Champagnon and M. Tomozawa: J. Appl. Phys. 103, (2008) 083506.
[24] F. L. Galeener: J. Non-Cryst. Solids 71, (1985) 373.
[25] R. B. Laughlin and J. D. Joannopoulos: Phys. Rev. B 16, (1977) 2942.

(Received: May 25, 2015, Accepted: January 26, 2016)